International Journal of Thermophysics, Vol. 14, No. 4, 1993

Thermal Effects in Compressible Viscous Flow in a Capillary[1]

H. R. van den Berg,[2] C. A. ten Seldam,[2] and P. S. van der Gulik[2]

Received January 14, 1993

The thermal effects for a compressible viscous flow in a capillary have been calculated by solving the equation of energy, where a parabolic profile is assumed for the axial flow velocity. It is shown that, in general, the temperature changes are small (a few millikelvins), consistent with the current assumption of an isothermal flow, except in the case of a critical, i.e., very compressible, fluid where the cooling can be substantial. This effect is demonstrated numerically on the basis of a flow of ethylene in nearly critical circumstances.

KEY WORDS: capillary flow; compressible flow; entry length; expansion cooling; temperature field; viscous dissipation.

1. INTRODUCTION

In a recent paper [1], a description of a "Compressible Laminar Flow in a Capillary" has been given, based on the three hydrodynamical equations of change, i.e., the equation of continuity, equation of motion, and equation of energy, and on an extensive set of conditions. One of these conditions states that the flow can be considered to be *isothermal*, implying that the energy equation can be ignored when solving the equation of motion.

In the present paper, an analytical solution for the equation of energy for a compressible flow is given, *independently* of the equation of motion, where a parabolic profile is assumed for the axial velocity. The final objective is to obtain information concerning the temperature distribution in the

[1] Paper dedicated to Professor Joseph Kestin.

[2] Van der Waals-Zeeman Laboratory, University of Amsterdam, Valckenierstraat 67, 1018 XE Amsterdam, The Netherlands.

840/14/4-17

fluid flowing in the capillary and to establish that the current premise of an isothermal flow in solving the equation of motion is generally consistent, except in the case of a critical, i.e., a very compressible, fluid. In the net thermal effect, two opposite contributions must be distinguished: the cooling part, due to expansion of a compressible fluid, and the heating part, due to viscous dissipation. An approximate solution for the cooling part in an ideal gas is given by Prud'homme et al. [2]. For an incompressible fluid, where only the heating part occurs, Brinkman [3] and Siegel et al. [4] calculated the thermal effect in the case of the boundary condition of a uniform wall heat flux. Brinkman also considered the case where the capillary-wall temperature is homogeneous. The latter boundary condition is also imposed on the present calculation for a compressible flow and was also used by van den Berg [5] in a numerical computation of the net temperature distribution.

In Section 2, the solutions of the equation of motion for a compressible laminar flow in a capillary are summarized, as far as they are relevant for solving the equation of energy. The equation of motion is solved in Ref. 1 by means of a perturbation method in successive orders in two parameters, of which the main one is a measure for the effect of the compressibility of the fluid. Van den Berg et al. [6] showed that, conditionally, this effect becomes substantial and has then to be accounted for, mainly by means of an additional factor in the classic Poiseuille formula for an incompressible fluid. This compression factor equals the ratio of a mean density in the capillary and the density at its entrance. The solution of the equation of energy, which is presented in Section 3 for the complete equation as well as for an approximated form, is split up into an asymptotic part and a part which decays exponentially with the axial coordinate. Furthermore, an entry length for the temperature is defined referring to the approach of the asymptotic value of the temperature. Finally, in Section 4 the formalism for the calculation of the thermal effect and of the corresponding entry length is applied to a flow of ethylene. This calculation shows that, in the vicinity of the gas–liquid critical point, the flow is far from isothermal due to the occurrence of substantial cooling.

The results of the present paper together with those given in Ref. 1 formed the base for the development of a reliable working equation for the capillary-flow viscometer. Consequently, a thorough comparison became possible between the results obtained with capillary viscometers and those obtained with other types of viscometers which are also suitable for absolute measurements, in particular with respect to the density dependence of the viscosity of various fluids. Among those other viscometers, the most important are the different versions of the oscillating disk/cup viscometer developed by Professor Kestin [7–9]. Another field

where the solution for the problem of compressible capillary flow can be applied is in the interpretation of experimental data in supercritical fluid chromatography and in other experiments with near-critical solvents [10].

2. HYDRODYNAMIC EQUATIONS AND CONDITIONS

A compressible capillary flow, generated by a force due to a static pressure p in the fluid, has been examined for a system without heat production by external sources. Therefore, the evolution of the density ρ, of the velocity $\vec{u}$, and of the internal energy $\hat{U}$ per unit mass in this system is described by the three hydrodynamical conservation equations.

Equation of continuity,

$$\frac{D\rho}{D\tau} = -\rho(\vec{\nabla} \cdot \vec{u}) \tag{1}$$

Equation of motion,

$$\rho \frac{D\vec{u}}{D\tau} = -\vec{\nabla} \cdot \vec{\vec{P}} \tag{2}$$

Equation of energy,

$$\rho \frac{D\hat{U}}{D\tau} = -(\vec{\nabla} \cdot \vec{q} + \vec{\vec{P}} : (\vec{\nabla}\vec{u})) \tag{3}$$

where τ is the time and $D/D\tau$ is an abbreviation for $\partial/\partial\tau + \vec{u} \cdot \vec{\nabla}$; $\vec{\vec{P}}$ is the pressure tensor and $\vec{q}$ is the heat-flow vector.

The solutions of these equations derived in this paper are restricted by the following assumptions: The fluid is Newtonian, which means that the pressure tensor can be written as

$$\vec{\vec{P}} = p\vec{\vec{I}} - 2\eta\vec{\vec{S}} - \kappa(\vec{\nabla} \cdot \vec{u})\,\vec{\vec{I}} \tag{4}$$

where η is the coefficient of shear viscosity of the fluid and κ the coefficient of bulk or dilatation viscosity, $\vec{\vec{I}}$ the unit tensor, and $\vec{\vec{S}}$ the rate of shear tensor defined by

$$\vec{\vec{S}} = \tfrac{1}{2}(\vec{\nabla}\vec{u} + (\vec{\nabla}\vec{u})^T) - \tfrac{1}{3}(\vec{\nabla} \cdot \vec{u})\,\vec{\vec{I}} \tag{5}$$

The radius R of the capillary is small compared to its length L (R/L is of the order 10^{-3}). The flow is stationary, laminar, and strictly axial; the Reynolds number Re ($=2R\rho\bar{u}/\eta$, with $\bar{u}$ the mean flow velocity) is less than about 2000. The pressure p is a function of z only (justified in Ref. 1 up to

second order in R/L). There is axial symmetry, no Knudsen flow, and no slip flow at the wall. There is no gravity effect and an influx correction can be neglected. The heat flux is linear with respect to the temperature gradient (law of Fourier $\vec{q} = -\lambda \vec{\nabla} T$, where λ is the coefficient of thermal conductivity) and the wall is at a homogeneous temperature T_0. The thermal conductivity and both viscosities of the fluid are constant in the pressure range throughout the capillary.

Along with the equation of state,

$$\rho = \rho(p, T) \tag{6}$$

and the boundary and initial conditions, Eqs. (1)–(5) give a complete determination of the distributions of pressure, density, temperature T, and velocity components in the flowing fluid. Substitution of Eq. (4) for the pressure tensor $\vec{\vec{P}}$ in the energy equation, Eq. (3), leads to four terms on the r.h.s. of that equation, which represent the increase in the internal energy of the system per unit time and unit volume due to, successively, the thermal conduction, the compression, and the dissipations related to the shear and bulk viscosity.

For the compressible flow through a straight circular capillary, the various equations are expressed in cylindrical coordinates (r, θ, z). Under the simplifying boundary conditions, the continuity equation, Eq. (1), then reduces to

$$\frac{\partial(\rho u_z)}{\partial z} = 0 \tag{7}$$

and the equation of motion, Eq. (2), for the axial velocity component to

$$\rho u_z \frac{\partial u_z}{\partial z} = -\frac{dp}{dz} + \eta \frac{1}{r} \frac{\partial}{\partial r}\left(r \frac{\partial u_z}{\partial r}\right) + \eta \left(\frac{4}{3} + \frac{\kappa}{\eta}\right) \frac{\partial^2 u_z}{\partial z^2} \tag{8}$$

In order to write the energy equation in terms of the temperature T, the internal energy is expressed in the enthalpy $\hat{H}$ according to $\hat{U} = \hat{H} - p/\rho$. Use of the continuity equation, Eq. (1), leads, then, to

$$\rho \frac{D\hat{H}}{D\tau} - \frac{Dp}{D\tau} = -\vec{\nabla} \cdot \vec{q} + (2\eta \vec{\vec{S}} + \kappa(\vec{\nabla} \cdot \vec{u})\, \vec{\vec{I}}) : \vec{\nabla} \vec{u} \tag{9}$$

and, with the first law of thermodynamics, to

$$\left(\rho \hat{C}_p \frac{\partial T}{\partial z} - T\alpha \frac{dp}{dz}\right) u_z = \lambda \left[\frac{1}{r} \frac{\partial}{\partial r}\left(r \frac{\partial T}{\partial r}\right) + \frac{\partial^2 T}{\partial z^2}\right] + \eta \left(\frac{\partial u_z}{\partial r}\right)^2 + \eta \left(\frac{4}{3} + \frac{\kappa}{\eta}\right)\left(\frac{\partial u_z}{\partial z}\right)^2 \tag{10}$$

$\hat{C}_p$ is the specific heat per unit mass at constant pressure and α is the thermal expansion coefficient,

$$\alpha = -\frac{1}{\rho}\left(\frac{\partial \rho}{\partial T}\right)_p \tag{11}$$

Since $p = p(z)$, the density ρ of the fluid is also only a function of z, under the preconception that radial density gradients due to temperature differences in the flow can be discarded. Integration of the continuity equation, Eq. (7), implies

$$u_z(x, z) = W\frac{E(x)}{\rho(z)} \tag{12}$$

where x is the reduced radial coordinate, $x = r/R$, and $E(x)$ is the velocity-profile function; the quantity W, which is independent of both z and x, is related to the mass-flow rate I according to

$$I = \int_0^R 2\pi r\, dr\, \rho(z)\, u_z(r, z) = 2\pi R^2 W \int_0^1 xE(x)\, dx \tag{13}$$

Equation (12) for $u_z(x, z)$ is inserted into Eq. (8), and a further simplification of this equation is carried out by integration over the length of the capillary, whereby the axial coordinate z crosses the interval $[0, L]$, the pressure $p(z)$ decreases from $p_b = p(0)$ to $p_{ex} = p(L)$, and the density $\rho(z)$ from $\rho_b = \rho(0)$ to $\rho_{ex} = \rho(L)$. The final result is then

$$C_1 E^2(x) - C_3 E(x) = 1 + C_2 \Im E(x) \tag{14a}$$

with the normalization and boundary conditions

$$E(0) = 1, \qquad E(1) = 0, \qquad \text{and} \qquad \left(\frac{dE}{dx}\right)_{x=0} = 0 \tag{14b}$$

where

$$\Im \text{ is the operator } \quad \frac{1}{x}\frac{\partial}{\partial x}\left(x\frac{\partial}{\partial x}\right) \tag{15}$$

and C_1, C_2, and C_3 are dimensionless constants, given by

$$C_1 = W^2\frac{Y}{X}, \qquad C_2 = \eta W\frac{L}{R^2}\frac{1}{X}, \qquad \text{and} \qquad C_3 = \eta\left(\frac{4}{3} + \frac{\kappa}{\eta}\right)W\frac{Z}{X} \tag{16}$$

The constants X, Y, and Z are defined by

$$X = \int_{p_{ex}}^{p_b} \rho \, dp = \langle \rho(p) \rangle \, \Delta p, \quad Y = \ln \frac{\rho_b}{\rho_{ex}}, \quad \text{and} \quad Z = \int_{\rho_{ex}}^{\rho_b} \rho d \left(\frac{1}{\rho^2} \frac{d\rho}{dz} \right) \tag{17}$$

where Δp $(= p_b - p_{ex})$ is the pressure difference over the capillary and $\langle \rho(p) \rangle$ a density calculated as the average of $\rho(p)$ over the pressure interval $[p_{ex}, p_b]$. The physical meaning of the key parameter C_1 was clarified in Ref. 1 by showing that C_1 can be written approximately as the product of some dimensionless quantities, originating from the dimensions of the capillary and properties of the fluid and the flow, namely,

$$C_1 \approx \frac{1}{4} \cdot \frac{R}{L} \cdot \mathrm{Re} \cdot \kappa_T \, \Delta p \tag{18}$$

where κ_T is the isothermal compressibility of the fluid.

The perturbation solution of Eqs. (14), in successive orders in parameter C_1, gives, in zero order for the velocity profile [1],

$$E(x) = E^{(0)}(x) = 1 - x^2 \tag{19}$$

and for the viscosity,

$$\eta = \eta^{(0)} = \frac{\pi R^4}{8IL} \rho_b \, \Delta p \, F_c \tag{20}$$

with

$$F_c = \frac{\langle \rho(p) \rangle}{\rho_b} \tag{21}$$

which is known as the compression factor.

For this zero-order parabolic velocity profile (19), Eq. (12) can be written as

$$u_z(x, z) = u_z^{(0)}(x, z) = 2\bar{u}(z)(1 - x^2) \tag{22}$$

By the use of Eq. (20), the mean flow velocity $\bar{u}(z)$ can be expressed as

$$\bar{u}(z) = \frac{I}{\pi R^2 \rho(z)} = \bar{u}_b \frac{\rho_b}{\rho(z)} \tag{23a}$$

with

$$\bar{u}_b = \bar{u}_{inc} F_c \qquad \text{and} \qquad \bar{u}_{inc} = \frac{R^2}{8\eta^{(0)}} \frac{\Delta p}{L} \tag{23b}$$

where $\bar{u}_b$ is the mean flow velocity at the beginning of the capillary for a compressible fluid and $\bar{u}_{inc}$ that for an incompressible fluid in the same circumstances.

3. THE TEMPERATURE DISTRIBUTION

3.1. Introduction

The temperature distribution $T(r, z)$ in a compressible viscous flow in a capillary is computed in zero order from the energy equation, Eq. (10). For this purpose, two additional assumptions are made. First, the axial velocity $u_z(r, z)$ is approximated by the zero-order solution of the equation of motion, Eq. (8). This solution, expressed by Eq. (22), includes the parabolic (Poiseuille) profile given by Eq. (19) and the mean velocity $\bar{u}(z)$ in Eqs. (23). It should be recalled here that higher-order contributions, due to the compressibility of the fluid, do not significantly affect the velocity profile [1]. Moreover, the impact of the velocity profile on the temperature distribution is only moderate, as shown in Section 3.4. Second, the pressure gradient dp/dz along the capillary is assumed to be constant:

$$\frac{dp}{dz} = -\frac{\Delta p}{L} \tag{24}$$

Furthermore, both the position coordinates r and z and the temperature $T(r, z)$ are reduced into dimensionless quantities, x, ζ, and $\theta(x, \zeta)$, respectively, by

$$x = \frac{r}{R}, \qquad \zeta = \frac{z}{R\,\mathrm{Pe}}, \qquad \theta(x, \zeta) = \frac{T(r, z) - T_0}{16\,\mathrm{Br}\,T_0} \tag{25}$$

where

$$\left.\begin{aligned} \mathrm{Pe}\ \text{is the Péclet number} &= \mathrm{RePr} \\ \mathrm{Re}\ \text{is the Reynolds number} &= \frac{2R\rho_b\bar{u}_b}{\eta} \\ \mathrm{Pr}\ \text{is the Prandtl number} &= \frac{\eta\hat{C}_p}{\lambda} = \frac{\nu}{D_T} \\ \mathrm{Br}\ \text{is the Brinkman number} &= \frac{\eta\bar{u}_{inc}^2}{\lambda T_0} \end{aligned}\right\} \tag{26}$$

Here $\nu = \eta/\rho$, the kinematic viscosity, and $D_T = \lambda/\rho \hat{C}_p$, the thermal diffusivity. By the use of Eqs. (20)–(25), Eq. (10) transforms into the nondimensional form

$$\left(\frac{\partial\theta}{\partial\zeta} + C\right)(1-x^2) = \Im\theta + \mathrm{Pe}^{-2}\frac{\partial^2\theta}{\partial\zeta^2} + x^2 + D(1-x^2)^2 \tag{27}$$

with the boundary conditions

$$\begin{aligned} &\text{at } x = 0, && \frac{\partial\theta}{\partial x} \equiv 0 \\ &\text{at } x = 1, && \theta(1,\zeta) \equiv 0 \\ &\text{at } \zeta = 0, && \theta(x,0) \equiv 0 \end{aligned} \tag{28}$$

and with the constants

$$C = T_0\alpha \tag{29}$$

$$D = \frac{1}{4}\left(\frac{4}{3} + \frac{\kappa}{\eta}\right)\left(\frac{R}{L}Y\right)^2 \tag{30}$$

The first boundary condition expresses the axial symmetry of the problem, the second implies that no accommodation effects are considered, so that the temperature of the fluid at the wall is equal to the homogeneous wall temperature T_0, and the third condition establishes that the fluid at the entrance of the capillary is also at equilibrium temperature over the whole cross-section. Actually, the quantities C and D vary slowly with the axial coordinate. Instead of these varying quantities, we have substituted in Eq. (27) their mean values over the length of the capillary. Therefore, in D the original factor $Ld\ln\rho(z)/dz$ is replaced by Y and, furthermore, in various terms the density $\rho(z)$ by the mean density $\langle\rho(z)\rangle$, which equals the mean density $\langle\rho(p)\rangle$, defined in Eq. (17), because of the constant pressure gradient (24).

The quantity C, originating from the compression term $-p(\vec{\nabla}\cdot\vec{u})$ in the energy equation, Eq. (3), and, therefore, a measure for the effect of the compressibility of the fluid, is considered as the key parameter in the reduced energy equation, Eq. (27). For an ideal gas $C = 1$, for a real gas in the critical region C is much larger than unity, for a dense gas $C < 1$, and for liquids $C \ll 1$. The term $\mathrm{Pe}^{-2}\,\partial^2\theta/\partial\zeta^2$ represents the energy rate per unit volume due to the heat conduction in the axial direction. The quantity Pe^2 is also treated as a parameter, although it is much less decisive. In many cases $\mathrm{Pe}^2 \gg 1$.

The solution $\theta(x, \zeta)$ of Eq. (27) is split into

$$\theta(x, \zeta) = C\theta_1(x, \zeta) + \theta_2(x, \zeta) \tag{31}$$

where $\theta_1(x, \zeta)$ and $\theta_2(x, \zeta)$ satisfy the equations

$$\frac{\partial \theta_1}{\partial \zeta}(1 - x^2) = \mathfrak{I}\theta_1 + \mathrm{Pe}^{-2}\frac{\partial^2 \theta_1}{\partial \zeta^2} + x^2 - 1 \tag{32}$$

$$\frac{\partial \theta_2}{\partial \zeta}(1 - x^2) = \mathfrak{I}\theta_2 + \mathrm{Pe}^{-2}\frac{\partial^2 \theta_2}{\partial \zeta^2} + x^2 + D(1 - x^2)^2 \tag{33}$$

and the boundary conditions given by Eq. (28). The function $\theta_1(x, \zeta)$ represents the reduced temperature in the case of cooling of the flowing fluid with $C = 1$, due to the expansion without viscous heat production, while $\theta_2(x, \zeta)$ describes the effect of viscous heating only. Consequently, the general solution $\theta(x, \zeta)$ of Eq. (27) is composed of the two particular solutions $\theta_n(x, \zeta)$. Actually, without the axial conduction term, Eq. (33) is the energy equation for an incompressible fluid ($D = 0$), with an axial coordinate $\zeta \hat{C}_p/\hat{C}_v$, as applied by Brinkman [3] for the calculation of the thermal effect due to viscous dissipation only.

3.2. The Asymptotic Solution

The asymptotic solutions for $\zeta \to \infty$ of Eqs. (32) and (33), $\theta_{n,\infty}(x) = \theta_n(x, \infty)$, are determined by imposing the condition that the axial derivatives of $\theta_n(x, \zeta)$ are identical to zero. For that case these equations reduce to

$$0 = \mathfrak{I}\theta_{1,\infty}(x) + x^2 - 1 \tag{34}$$

$$0 = \mathfrak{I}\theta_{2,\infty}(x) + x^2 + D(1 - x^2)^2 \tag{35}$$

with the boundary conditions

$$\begin{aligned} &\text{at } x = 0, \qquad \frac{\partial \theta_{n,\infty}(x)}{\partial x} = 0 \\ &\text{at } x = 1, \qquad \theta_{n,\infty}(x) = 0 \end{aligned} \tag{36}$$

The solutions are easily found by repeated integration as

$$\theta_{1,\infty}(x) = -\frac{1}{16}(3 - 4x^2 + x^4) \tag{37}$$

$$\theta_{2,\infty}(x) = \frac{1}{16}(1 - x^4) + \frac{D}{72}(1 - x^2)(11 - 7x^2 + 2x^4) \tag{38}$$

The second term in this expression for the viscous-heating contribution $\theta_{2,\infty}(x)$ contains in the constant D the ratio κ/η of the bulk and shear viscosity. In experiments, Madigosky [11] found values up to 0.7 in dense gaseous argon for this ratio. From experimental data on water and a number of organic liquids, Karim and Rosenhead [12] deduced that the value of this viscosity ratio ranges from about 1 to 120. On the basis of these conclusions, we estimate that the second term in $\theta_{2,\infty}(x)$ is smaller than 0.01% of the first term, on the condition that $R/L \leqslant 10^{-3}$ and $Y \leqslant 1$. Henceforth, we omit this term, which implies that the impact of the bulk viscosity on the thermal effect is neglected. The total asymptotic solution $\theta_\infty(x)$ is then

$$\theta_\infty(x) = -\frac{1}{16}[C(3-4x^2+x^4)-(1-x^4)] \tag{39}$$

so that the temperature change on the axis is given by

$$T(0,\infty)-T_0 = -\mathrm{Br}\ T_0(3C-1) = -\frac{\eta \bar{u}_{\mathrm{inc}}^2}{\lambda}(3T_0\alpha-1) \tag{40}$$

3.3. The Solution for Finite ζ

In order to solve Eqs. (32) and (33) for finite ζ, each of the functions $\theta_n(x,\zeta)$ is written as the sum of the corresponding asymptotic solution given in the preceding section and a function $\theta_{n,d}(x,\zeta)$, which will be damped out exponentially with ζ and which must be determined:

$$\theta_n(x,\zeta) = \theta_{n,\infty}(x) + \theta_{n,d}(x,\zeta) \qquad \text{for} \quad n=1,2 \tag{41}$$

In both cases substitution leads to the equation

$$\frac{\partial\theta_{n,d}}{\partial\zeta}(1-x^2) = \mathfrak{I}\theta_{n,d} + \mathrm{Pe}^{-2}\frac{\partial^2\theta_{n,d}}{\partial\zeta^2} \tag{42}$$

with the four boundary conditions

$$\begin{aligned}
&\text{at } x=0, && \frac{\partial\theta_{n,d}(x,\zeta)}{\partial x} \equiv 0\\
&\text{at } x=1, && \theta_{n,d}(1,\zeta) \equiv 0\\
&\text{at } \zeta=0, && \theta_{n,d}(x,0) \equiv -\theta_{n,\infty}(x)\\
&\text{at } \zeta=\infty, && \theta_{n,d}(x,\infty) \equiv 0
\end{aligned} \tag{43}$$

The fourth condition ascertains that the damping term vanishes in the asymptotic limit.

If the functions $\theta_{n,d}(x, \zeta)$ are assumed to be of the form

$$\theta_{n,d}(x, \zeta) = \Psi_n(x)\, \Phi_n(\zeta) \tag{44}$$

then Eq. (42) leads for $\Phi_n(\zeta)$ to an exponential dependence on the axial coordinate,

$$\Phi_n(\zeta) = e^{-\beta^2 \zeta} \tag{45}$$

which satisfies the fourth boundary condition in Eq. (43), and for $\Psi_n(x)$ to an ordinary differential equation:

$$\Im \Psi_n + \beta^2 (1 + \mathrm{Pe}^{-2}\beta^2 - x^2)\, \Psi_n = 0 \tag{46}$$

In combination with the first and second boundary condition, this equation for the radial dependence of the temperature distribution has an infinite number of eigenvalues $\beta_i^2 = \beta_i^2(\mathrm{Pe}^2)$ and corresponding eigenfunctions $\psi_i(x)$ $(i = 1, 2, \ldots)$, independent of n, which produce the general solution

$$\Psi_n(x) = \sum_{i=1}^{\infty} b_{n,i} \psi_i(x) \tag{47}$$

The eigenfunctions can be developed in the power series

$$\psi_i(x) = \sum_{k=0}^{\infty} c_{k,i} x^{2k} \tag{48}$$

of which the permanent convergence is ensured by the recursion formulas for the coefficients:

$$\begin{aligned} c_{1,i} &= -\frac{\beta_i^2}{4} (1 + \mathrm{Pe}^{-2}\beta_i^2)\, c_{0,i} \\ c_{k,i} &= -\frac{\beta_i^2}{4k^2} [(1 + \mathrm{Pe}^{-2}\beta_i^2)\, c_{k-1,i} - c_{k-2,i}] \qquad \text{for} \quad k \geqslant 2 \end{aligned} \tag{49}$$

We make (arbitrarily) $\psi_i(0) = 1$ by choosing $c_{0,i} = 1$. Each of the eigenfunctions ψ_i satisfies the first boundary condition in Eq. (43), because these solutions are even functions. The second condition requires that

$$S \equiv \psi_i(1) = \sum_{k=0}^{\infty} c_{k,i} = 0 \tag{50}$$

Since $c_{k,i} = c_{k,i}(\beta_i^2)$, the eigenvalues β_i^2 are the zeros of the sum S of the coefficients $c_{k,i}$. These zeros, and simultaneously the coefficients $c_{k,i}$, can be readily computed by brute force: let β_i^2 run through the integers 1, 2, 3,..., and determine whenever S has changed sign. In this way one obtains the zeros β_i^2 in the order of increasing value for $i = 1, 2, \ldots$. We have carried out this calculation for $\mathrm{Pe}^2 = \infty$, 1000, 100, 10, and 1. It turns out that in each of these five cases the coefficients $c_{k,i}$, calculated with the formula's of Eq. (49) for each fixed eigenvalue β_i^2 and for running k, are positive for even k and negative for odd k and, furthermore, that $|c_{k,i}|$ goes through a maximum and then falls monotonously. Since the $\max_k |c_{k,i}|$ with increasing β_i^2 increases very strongly (in the case $\mathrm{Pe}^2 = \infty$ from 1.8 at $i = 1$ for $k = 1$ to 3.1×10^{12} at $i = 8$ for $k = 20$, and in the case $\mathrm{Pe}^2 = 1$ from 1.6 at $i = 1$ for $k = 1$ to 6.6×10^{8} at $i = 8$ for $k = 12$), the computation of the eigenvalues cannot be extended indefinitely; with 18-digit accuracy we succeeded in computing the first *eight* zeros, which are given in Tables I A–E together with the number of coefficients $c_{k,i}$ involved. This number is determined by the limiting condition applied, *viz.*, the computation is truncated every time for that value of k for which $|c_{k,i}| < \max_k |c_{k,i}| \times 10^{-12}$. Due to the accuracy of the computation, the values of the sum S, calculated with Eq. (50) for each of the zeros β_i^2, are not exactly zero, as they should be. The deviations are smaller than 10^{-10} in nearly all cases.

With the polynomials, Eq. (48), calculated for the eigenfunctions ψ_i, the coefficients $b_{n,i}$ in expansion, Eq. (47), for the general solutions Ψ_n can be determined from the third boundary condition:

$$\sum_{i=1}^{m} b_{n,i}\psi_i(x) = -\theta_{n,\infty}(x) \qquad \text{for} \quad n = 1, 2, \text{ and } m = 8 \tag{51}$$

where the asymptotic solutions $\theta_{1,\infty}(x)$ and $\theta_{2,\infty}(x)$ are given by Eqs. (37) and (38) without the second viscous dissipation term ($D = 0$).

For the actual calculation of the coefficients $b_{n,i}$, a practical method has been applied, which satisfied the condition given by Eq. (51) approximately, i.e., precisely in m points. For this purpose m values of x are substituted in both sides of this equation, arbitrarily chosen in the interval [0, 1]. We choose m equidistant values of x from 0 to $(m-1)/m$. The coefficients $b_{n,i}$ must then be solved from a set of m linear equations for each of the five values of Pe^2. The resulting values of $b_{n,i}$, for $n = 1, 2$ and $i = 1, \ldots, m$, are also given in Tables I A–E. We note that the functions $\Psi_n(x) + \theta_{n,\infty}(x)$ for $n = 1, 2$, which should be identical to zero, oscillate around this value due to the use of a finite number of eigenfunctions. The method presented yields the maximum absolute deviation for $\mathrm{Pe}^2 = \infty$, *viz.*, 0.0001 for $n = 1$ and 0.0011 for $n = 2$.

Table I. Eigenvalues, Mean Values of Eigenfunctions, and Coefficients for the Solution of the Energy Equation in Terms of the Temperature

i	β_i^2	N^a	$b_{1,i}$	$b_{2,i}$	$\bar{\psi}_i$
			(A) $Pe^2 = \infty$		
1	7.31359	17	0.201876	−0.084593	0.393597
2	44.60946	26	−0.018081	0.031577	−0.165943
3	113.92103	32	0.005170	−0.014529	0.105110
4	215.24054	38	−0.002260	0.008642	−0.076931
5	348.56432	44	0.001183	−0.005483	0.060675
6	513.92624	49	−0.000599	0.003024	−0.050079
7	717.27568	54	0.000874	0.005988	0.040546
8	869.09814	58	−0.000665	0.004850	−0.037520
			(B) $Pe^2 = 1000$		
1	7.24785	17	0.201977	0.084996	0.393911
2	42.03430	25	−0.018228	0.032456	−0.164861
3	98.87895	31	0.005220	0.015503	0.101023
4	169.66928	36	−0.002165	0.009061	−0.069431
5	248.87920	41	0.001040	0.005673	0.050215
6	333.33022	45	−0.000543	0.003769	−0.037499
7	421.29458	48	0.000341	−0.002985	0.028746
8	516.11709	51	−0.000142	0.001371	−0.022171
			(C) $Pe^2 = 100$		
1	6.74405	17	0.201959	−0.086225	0.396330
2	30.76792	24	−0.017757	0.033991	−0.158369
3	59.50346	28	0.004313	−0.015383	0.087138
4	89.47668	32	−0.001380	0.007891	−0.054177
5	119.97261	35	0.000511	−0.004352	0.036760
6	150.75031	38	−0.000213	0.002535	−0.026670
7	182.69735	41	0.000093	−0.001425	0.020355
8	212.73725	44	−0.000027	0.000468	−0.016140
			(D) $Pe^2 = 10$		
1	4.62589	16	0.199457	0.087017	0.406831
2	14.36583	21	−0.013858	0.033607	−0.143040
3	24.21902	25	0.002351	−0.013142	0.072495
4	34.10340	28	−0.000591	0.006137	−0.044452
5	44.00496	31	0.000195	0.003244	0.030557
6	53.91644	33	−0.000077	0.001817	−0.022597
7	63.83411	36	0.000031	0.000931	0.017564
8	73.75650	39	−0.000008	0.000274	−0.014152
			(E) $Pe^2 = 1$		
1	2.04437	14	0.195275	−0.086344	0.420388
2	5.18734	18	−0.008751	0.031901	−0.131103
3	8.32345	22	0.001194	−0.011589	0.065986
4	11.46137	25	−0.000286	0.005358	−0.041023
5	14.60050	28	0.000095	−0.002846	0.028572
6	17.74037	31	−0.000038	0.001588	−0.021344
7	20.88069	34	0.000015	−0.000793	0.016719
8	24.02099	36	−0.000004	0.000225	−0.013551

[a] N is the number of coefficients $c_{k,i}$.

Where $Pe^2 = \infty$, the differential equation, Eq. (46), is of the Sturm–Liouville type. This allows us to apply a mathematically more sophisticated method to compute $b_{n,i}$, where use is made of the fact that the eigenfunctions $\{\psi_i(x)\}_{i=1}^{\infty}$ form an orthogonal system on the interval $[0, 1]$ with the weight function $x(1-x^2)$. This leads to

$$b_{n,i} = -\frac{\int_0^1 \theta_{n,\infty}(x)\,\psi_i(x)\,x(1-x^2)\,dx}{\int_0^1 \psi_i^2(x)\,x(1-x^2)\,dx} \tag{52}$$

Due to lack of computational accuracy, however, this method broke down for the coefficients $b_{n,i}$ with $i > 4$, even when extended reals were used; the polynomials ψ_i consist of a large number (17 for ψ_1 up to 58 for ψ_8) of alternating terms with large coefficients $c_{k,i}$, which, furthermore, occur squared in the denominator of Eq. (52). It turns out that the coefficients $b_{n,1}, \ldots, b_{n,4}$ calculated with Eq. (52) agree reasonably well with those obtained according to the above-mentioned practical method, which are given in Table IA.

According to Eqs. (31) and (41), the total solution of Eq. (27) for the temperature distribution $\theta(x, \zeta)$ can now be written as

$$\theta(x,\zeta) = -\frac{1}{16}\left[C(3-4x^2+x^4)-(1-x^4)\right] + \sum_{i=1}^{8} (Cb_{1,i}+b_{2,i})\,\psi_i(x)\,e^{-\beta_i^2\zeta} \tag{53}$$

In Fig. 1 the temperature distribution in a capillary across the radial direction, where $Pe^2 = \infty$, is presented for four different values of the axial coordinate ζ, including the asymptotic limit. The two separate contributions, *viz.*, the cooling part $\theta_1(x, \zeta)$ and the viscous heating part $\theta_2(x, \zeta)$, are shown in Fig. 1a, and the net effect $\theta(x, \zeta)$ for $C = 1$ is shown in Fig. 1b. The curves for $\theta_2(x, \zeta)$ agree with those given by Brinkman [3] as the result of his treatment of the heat effects in an incompressible capillary flow under the same conditions as applied in the present calculation. Making this comparison, one should take into account that the Brinkman results are expressed in a different reduced temperature which equals 4θ. He calculated the eigenvalues β_1^2 to β_4^2 in four digits. These values are equal to those given in Table IA, except for that of β_4^2, which shows a difference of 0.6%.

Figures 2a and b contain the calculated temperature distributions versus the axial coordinate ζ for $Pe^2 = \infty$ along five different lines of constant x.

From Figs. 1 and 2, where $Pe^2 = \infty$, it can be seen clearly that, close to the wall of the capillary where the velocity gradient $\partial u_z/\partial x$ reaches its

maximum value, a positive net temperature effect even arises due to the strong viscous dissipation. Similar figures can be obtained for smaller values of Pe^2. Figure 3 shows the temperature distribution versus the axial coordinate ζ along the center line $x = 0$ for $Pe^2 = \infty$, 10, and 1. The composing parts $\theta_1(0, \zeta)$ and $\theta_2(0, \zeta)$ are given in Fig. 3a, and the net effect $\theta(0, \zeta)$ for $C = 1$ in Fig. 3b. The curves for $Pe^2 = 1000$ and 100 nearly coincide with the limiting curve for $Pe^2 = \infty$ and are therefore omitted. In these figures the ζ axis is extended to 1.5 because of the slower course of $\theta(0, \zeta)$ for smaller values of Pe^2.

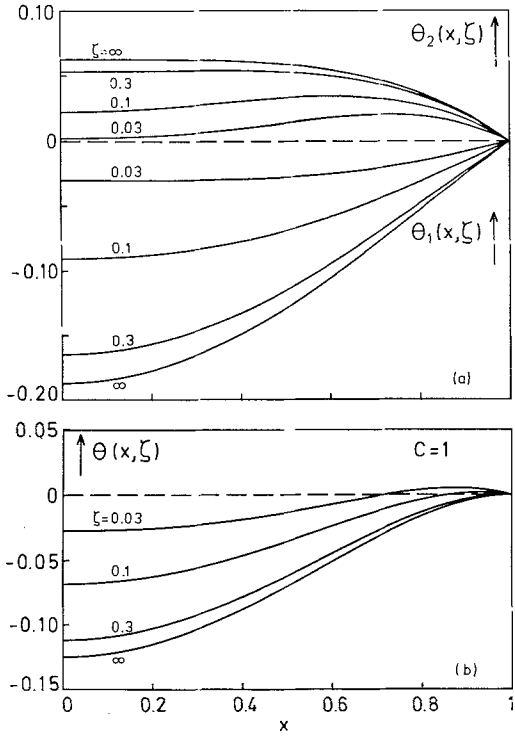

Fig. 1. The reduced temperature for compressible viscous flow in a capillary versus the reduced radial coordinate, along four lines of constant reduced axial coordinate ζ for $Pe^2 = \infty$. (a) The cooling contribution $\theta_1(x, \zeta)$, due to expansion, and the heating contribution $\theta_2(x, \zeta)$, due to viscous dissipation. (b) The net temperature effect $\theta(x, \zeta)$, calculated for compressibility parameter $C = 1$.

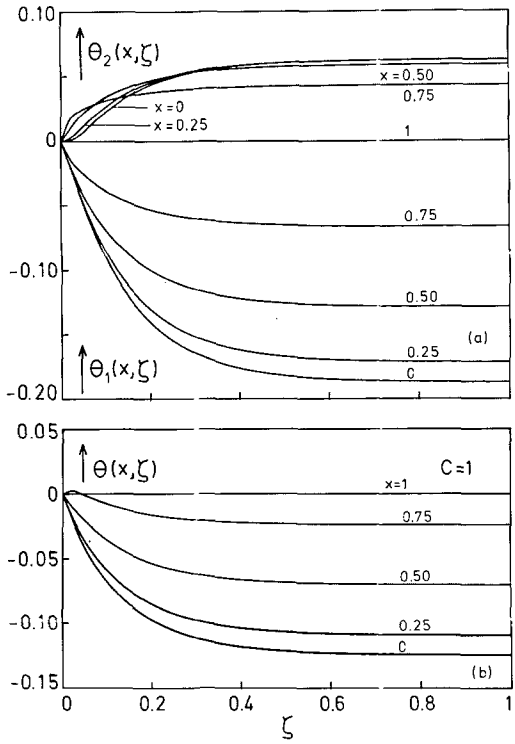

Fig. 2. The reduced temperature for compressible viscous flow in a capillary versus the reduced axial coordinate, along five lines of constant reduced radial coordinate x for $\mathrm{Pe}^2 = \infty$. (a) The cooling contribution $\theta_1(x, \zeta)$, due to expansion, and the heating contribution $\theta_2(x, \zeta)$, due to viscous dissipation. (b) The net temperature effect $\theta(x, \zeta)$, calculated for compressibility parameter $C = 1$.

3.4. Approximate Solution for Finite ζ

In order to examine the influence of the velocity profile on the temperature damping term $\theta_{n,d}(x, \zeta)$, Eq. (42) is solved for the case $\mathrm{Pe}^2 = \infty$ with an uniform velocity profile that is obtained by replacement of the parabolic velocity profile $(1 - x^2)$ by its mean value $\frac{1}{2}$. With unchanged boundary conditions given by Eq. (43) and separating, as in Eq. (44), the x and ζ dependence of the approximate damping $\theta_{a,d}$, Eqs. (45) and (46) now become

$$\Phi_n(\zeta) = e^{-2\alpha^2\zeta} \tag{54}$$

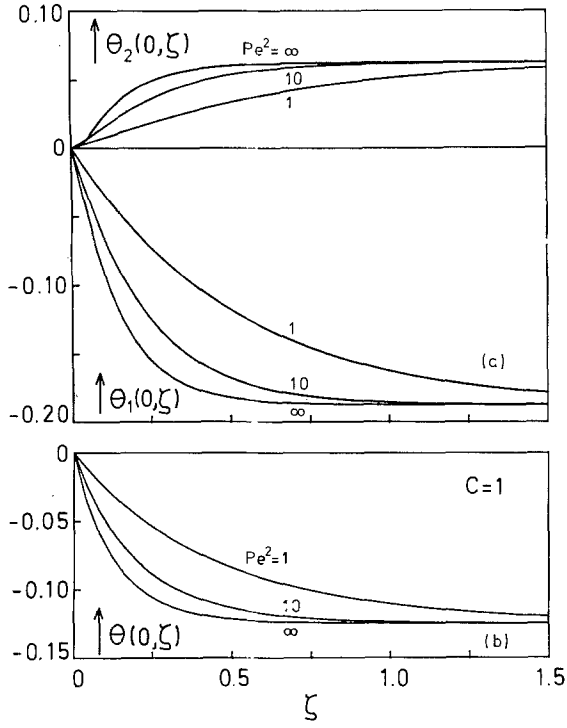

Fig. 3. The reduced temperature for compressible viscous flow in a capillary versus the reduced axial coordinate, along the axis ($x=0$) for $Pe^2=\infty$, 10, and 1. (a) The cooling contribution $\theta_1(0,\zeta)$, due to expansion, and the heating contribution $\theta_2(0,\zeta)$, due to viscous dissipation. (b) The net temperature effect $\theta(0,\zeta)$, calculated for compressibility parameter $C=1$.

and

$$\mathfrak{F}\Psi_n+\alpha^2\Psi_n=0 \tag{55}$$

The latter is the zero-order Bessel differential equation. In combination with the first two boundary conditions given by Eq. (43), this equation has an infinite number of eigenvalues α_i^2 and corresponding eigenfunctions $\psi_i(\alpha_i x)$ ($i=1,2,...$), independent of n. Each of these functions is a linear combination of the zero-order Bessel function $J_0(\alpha_i x)$ and the zero-order Neumann function $N_0(\alpha_i x)$. However, since $\psi_i(0)$ must be finite and

$N_0(\alpha_i x)$ tends to minus infinity for x approaching zero, the coefficient of the function $N_0(\alpha_i x)$ must be zero. The general solution is therefore

$$\Psi_n(x) = \sum_{i=1}^{\infty} a_{n,i} J_0(\alpha_i x) \tag{56}$$

Each of the functions $J_0(\alpha_i x)$ is even and thus satisfies the first boundary condition in Eq. (43). The fulfillment of the second boundary condition at $x = 1$ requires

$$J_0(\alpha_i) = 0 \qquad \text{for} \quad i = 1, 2, \ldots \tag{57}$$

which means that the eigenvalues α_i are the known positive zeros of the zero-order Bessel function. In analogy with the coefficients $b_{n,i}$ in Eq. (47), the coefficients $a_{n,i}$ in Eq. (56) can be found from the third boundary condition at $\zeta = 0$:

$$\sum_{i=1}^{\infty} a_{n,i} J_0(\alpha_i x) = -\theta_{n,\infty}(x) \qquad \text{for} \quad n = 1, 2 \tag{58}$$

Because of the orthogonality of the functions $\{J_0(\alpha_i x)\}_{i=1}^{\infty}$ on the interval $[0, 1]$ with the weight function x, we can write

$$a_{n,i} = -\frac{\int_0^1 \theta_{n,\infty}(x)\, J_0(\alpha_i x)\, x\, dx}{\int_0^1 J_0^2(\alpha_i x)\, x\, dx} \tag{59}$$

Substitution of the asymptotic solutions $\theta_{1,\infty}(x)$ and $\theta_{2,\infty}(x)$, as given by Eqs. (37) and (38), and use of some properties of the Bessel functions of zero and first order (see Appendix), leads straightforwardly to

$$\begin{aligned} a_{1,i} &= \frac{8}{\alpha_i^5 J_1(\alpha_i)} \\ a_{2,i} &= -\frac{2}{\alpha_i^5 J_1(\alpha_i)} (\alpha_i^2 - 4) \end{aligned} \tag{60}$$

The total approximate solution $\theta_a(x, \zeta)$ is then

$$\begin{aligned} \theta_a(x, \zeta) = &-\frac{1}{16} [C(3 - 4x^2 + x^4) - (1 - x^4)] \\ &+ 8 \sum_{i=1}^{\infty} \frac{J_0(\alpha_i x)}{\alpha_i^5 J_1(\alpha_i)} \left[C - \frac{1}{4} (\alpha_i^2 - 4) \right] e^{-2\alpha_i^2 \zeta} \end{aligned} \tag{61}$$

It turns out that the resulting curves for $\theta_a(x, \zeta)$ versus x for constant ζ and versus ζ for constant x are globally the same as those for $\theta(x, \zeta)$ in Figs. 1 and 2. For the approximate solution, the dependence on x and ζ is only somewhat stronger. Therefore, it can be stated that the influence of the velocity profile on $\theta_{n,d}(x, \zeta)$ is limited.

3.5. Mean Temperature $\bar{\theta}(\zeta)$

For practical applications, it can be convenient to use the mean temperature $\bar{\theta}(\zeta)$, which is calculated from $\theta(x, \zeta)$ by averaging over the cross section of the capillary according to

$$\bar{\theta}(\zeta) = 2 \int_0^1 x\theta(x, \zeta)\, dx \tag{62}$$

From Eq. (53) it then follows that

$$\bar{\theta}(\zeta) = -\frac{1}{24}(2C-1) + \sum_{i=1}^{8} (Cb_{1,i} + b_{2,i})\, \bar{\psi}_i\, e^{\beta_i^2 \zeta} \tag{63}$$

The mean $\bar{\psi}_i$ values are calculated from the polynomial expansion, Eq. (48), as

$$\bar{\psi}_i = \sum_{k=0}^{\infty} \frac{1}{k+1} c_{k,i}(\beta_i^2) \tag{64}$$

These values are also inserted in Tables IA–E and we can see that, appropriately, $b_{1,i}\bar{\psi}_i > 0$ and $b_{2,i}\bar{\psi}_i < 0$ for all values of i.

From Eq. (61), the approximate mean temperature $\bar{\theta}_a(\zeta)$, with the same asymptotical limit as $\bar{\theta}(\zeta)$, is found to be

$$\bar{\theta}_a(\zeta) = -\frac{1}{24}(2C-1) + 16 \sum_{i=1}^{\infty} \frac{1}{\alpha_i^6} \left[C - \frac{1}{4}(\alpha_i^2 - 4) \right] e^{2\alpha_i^2 \zeta} \tag{65}$$

In Fig. 4 the mean reduced temperature versus the axial coordinate ζ is presented by solid lines and the approximate mean reduced temperature by dashed lines, where $\mathrm{Pe}^2 = \infty$, 10, and 1. The composing parts $\bar{\theta}_1(\zeta)$ and $\bar{\theta}_{1a}(\zeta)$, for the cooling of the fluid due to expansion, and $\bar{\theta}_2(\zeta)$ and $\bar{\theta}_{2a}(\zeta)$, for the heating due to viscous dissipation, are shown in Fig. 4a, and the net effect $\bar{\theta}(\zeta)$ and $\bar{\theta}_a(\zeta)$ for $C = 0$, 0.42, 0.50, and 1 in Fig. 4b. For $C = 0.42$ and 0.50, only the curves corresponding to $\mathrm{Pe}^2 = \infty$ are shown. For these C

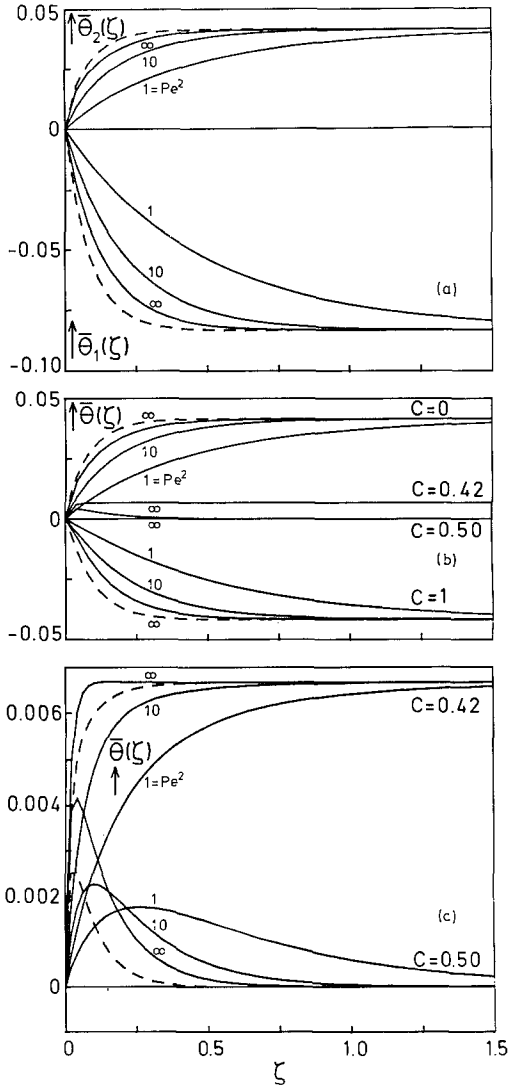

Fig. 4. The mean reduced temperature for compressible viscous flow in a capillary versus the reduced axial coordinate. (——) Solution for parabolic flow velocity profile for $Pe^2 = \infty$, 10, and 1. (---) Solution for uniform flow velocity profile for $Pe^2 = \infty$. (a) The cooling contribution $\bar{\theta}_1(\zeta)$, due to expansion, and the heating contribution $\bar{\theta}_2(\zeta)$, due to viscous dissipation. (b) The net temperature effect $\bar{\theta}(\zeta)$, calculated for compressibility parameter $C = 0$, 0.42, 0.5, and 1. (c) Enlargement of b for $C = 0.42$ and 0.5.

values the contribution of the cooling nearly counterbalances that of the heating. More details of the axial dependence of the temperature in these cases for all three values of Pe^2 can be read from Fig. 4c, in which the vertical scale is 18.75 times larger than in Figs. 4a and b. For $Pe^2 = \infty$ the function $\bar{\theta}(\zeta)$ increases monotonously for $0 \leqslant C < 0.42$, goes through a maximum for $0.42 < C < 0.91$, and decreases monotonously for $C \geqslant 0.91$ because of the preponderance of the expansion term. For the smaller values of Pe^2 the picture is nearly the same, with only a small shift in the bounds for C. Furthermore, it is clear that, in spite of the magnitude of the change in the velocity profile, from parabolic to uniform, its effect on the axial dependence of the mean temperature is not really spectacular. Since it is shown in Ref. 1 that, depending on the parameter C_1 in Eq. (14a), the higher-order velocity profile deviates only slightly from the parabolic profile, we may conclude that the real course of the mean temperature will not differ substantially from that given by Eq. (63) for $\bar{\theta}(\zeta)$. We can conclude also that the solutions $\bar{\theta}(\zeta)$ for $Pe^2 = 10$ and 1 deviate significantly from those for $Pe^2 = \infty$. The latter represent the solutions of Eq. (27) neglecting the axial conduction term, as was usually done in the past.

Prud'homme et al. [2] analyzed the process of cooling in the flow of an ideal gas ($C = 1$) without viscous heating and without axial conduction, starting from Eq. (32) for $\theta_1(x, \zeta)$. These authors simplify this equation by the immediate elimination of the radial dependence of the temperature, which is achieved by averaging of the equation over the cross section of the capillary. Furthermore, they introduce an unspecified heat-transfer coefficient h in the radial heat conduction at the wall of the capillary. The condition that their solution has the same asymptotic limit $-\frac{1}{12}$ as that given by our Eq. (63) leads to $h = 3\lambda/R$, corresponding with a Nusselt number of 6. The result for the mean temperature $\bar{\theta}_p(\zeta)$ is then $\bar{\theta}_p(\zeta) = -(1/12)$ $[1 - \exp(-12\zeta)]$. It turns out that the curve for $\bar{\theta}_p(\zeta)$ nearly coincides with that for $\bar{\theta}_{1a}(\zeta)$ in Fig. 4a. This is understandable since the coefficient $2\alpha_1^2$ in the exponent of Eq. (65) equals about 11.6, while the next term with $2\alpha_2^2 \approx 60.9$ is almost negligible.

3.6. Entry Length

In analogy with the entry length for the velocity, a transition length ζ_{99} for the mean temperature $\bar{\theta}(\zeta)$ is introduced. In order to be independent of the parameter C, ζ_{99} is defined as that value of ζ for which $\bar{\theta}_1(\zeta)$ reaches 99% of its asymptotic value $\bar{\theta}_1(\infty) = -1/12$. It then turns out that $\bar{\theta}_2(\zeta_{99}) = (0.99 + \varepsilon)\,\bar{\theta}_2(\infty)$, in which the value of ε varies from 0.0012 to 0.0017, depending on the value of Pe. The value of ζ_{99} is found to be nearly

constant for $\mathrm{Pe} > 50$ and to increase with decreasing values of Pe for $\mathrm{Pe} < 50$, especially for $\mathrm{Pe} < 10$. This behavior is expressed by

$$\zeta_{99} = \begin{cases} 0.625 & \text{for} \quad \mathrm{Pe} > 50 \\ 0.625 + 0.138\, e^{-0.099\,\mathrm{Pe}} + 3.329\, e^{\,0.8\,\mathrm{Pe}} \\ \quad \text{to within } 0.1\,\% \text{ for } 1 \leqslant \mathrm{Pe} \leqslant 50 \end{cases} \tag{66}$$

For $\bar{\theta}(\zeta_{99})$ the relation

$$\bar{\theta}(\zeta_{99}) = 0.99\, \bar{\theta}(\infty) + \varepsilon \bar{\theta}_2(\infty) \tag{67}$$

then holds, i.e., $\bar{\theta}(\zeta_{99})$ equals 99% of $\bar{\theta}(\infty)$ plus a bias which is, at most, 0.17% of $\bar{\theta}_2(\infty)$, which is about 7×10^{-5}. Consequently, for almost all values of C the reduced temperature $\bar{\theta}(\zeta_{99})$ equals practically 99% of the asymptotic value $\bar{\theta}(\infty)$. This percentage can be substantially different, only for C values around 0.5, where $\bar{\theta}(\infty) \cong 0$. However, in that small range of C values, the net thermal effect is very small (see Figs. 4b and c), so that for these circumstances the practical meaning of the entry length is restricted anyhow. If ΔL_{T} is the real distance in the capillary corresponding to the entry length ζ_{99}, according to Eq. (25) we can write

$$\Delta L_{\mathrm{T}} = \zeta_{99} R\, \mathrm{Pe} \tag{68}$$

The increase in ΔL_{T} with the Péclet number can be understood in view of the fact that it is possible to interpret Pe as the ratio of the axial heat transport by convection and by conduction. If the entry length is referred to the temperature on the axis $\theta(0, \zeta)$, then ζ_{99} must be determined from $\theta_2(0, \zeta)$ and is also found to be constant for $\mathrm{Pe} > 50$ with the value 0.672.

The entry length ΔL_{u} for the center-line velocity is $\Delta L_{\mathrm{u}} = 0.11\, R\, \mathrm{Re}$ as calculated by Langhaar [13], Hornbeck [14], and many others. The ratio of the entry lengths for temperature and velocity, $\Delta L_{\mathrm{T}}/\Delta L_{\mathrm{u}} \approx 6\, \mathrm{Pr}$, therefore, depends only on thermophysical properties of the fluid and not on the flow itself.

In Fig. 5, the net mean reduced temperature is plotted versus the logarithm of the ratio of the real axial coordinate z and the length of the capillary L for $R/L = 0.001$, and for eight values of Pe^2, *viz.*, $\mathrm{Pe}^2 = 10^7$, 10^6,..., 10^0. By plotting $\bar{\theta}$ as a function of $\log(z/L)$ instead of as a function of the reduced coordinate ζ (as in Fig. 4), the curves, which nearly coincided for $\mathrm{Pe} > 10$, transform now into parallel and equidistant but no longer coincident curves, due to the occurrence of the factor Pe in the transformation of ζ into z. Figure 5a refers to values for the parameter C of 0.42 and 0.50, and Fig. 5b, where the vertical scale is 6.25 times smaller,

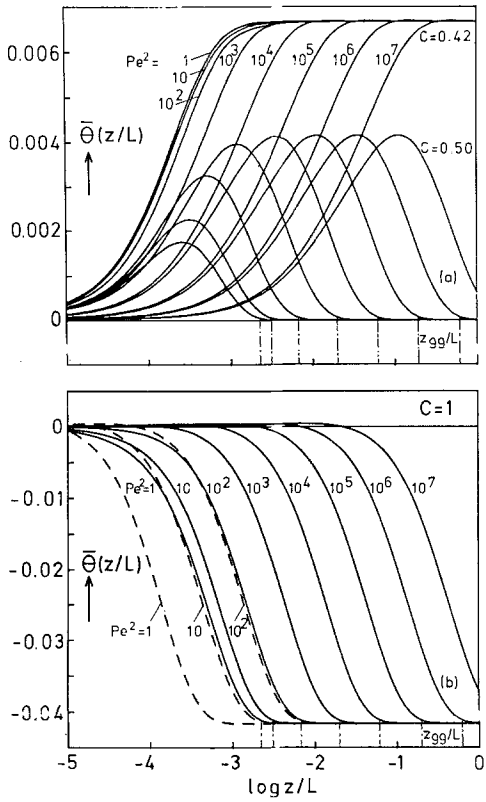

Fig. 5. The net mean reduced temperature and the entry length z_{99} for compressible viscous flow in a capillary ($R/L = 0.001$) versus the axial coordinate on a logarithmic scale, for eight values of the Péclet number at three values of the compressibility parameter C. (a) $C = 0.42$ and $C = 0.50$. (b) $C = 1$; (---) solution with neglect of axial conduction.

to $C = 1$. With a different value for R/L, *all* the curves in Fig. 5 are parallelly shifted over the same distance.

In the two figures, Figs. 5a and b, the entry lengths z_{99}/L, which are independent of C, are also indicated. It is obvious that for the smaller values of Pe ($\mathrm{Pe} < 10$), where the influence of axial heat conduction dominates over that of convection, the entry length is less than 1% of the length of the capillary, which means that the asymptotic temperature is reached almost instantly.

If $\bar{\theta}(\zeta)$ is calculated for $\mathrm{Pe}^2 = \infty$, i.e., neglecting the axial conduction term in Eq. (42), and subsequently different values of Pe ($\mathrm{Pe}^2 = 1$, 10, and

100) are used in the transformation $\zeta \to z/L$ only, then the dashed lines in Fig. 5b are obtained. From these approximate solutions it can also be seen that the axial conduction for $\mathrm{Pe} > 10$ can be ignored as far as practical purposes are concerned.

4. APPLICATION

Finally, it will be shown that, conditionally, the thermal effects in a compressible capillary flow are significant. For the mean reduced temperature, it follows from Eq. (63) that the difference between the mean asymptotic real temperature $\bar{T}(\infty)$ and the wall temperature T_0 is given by

$$\bar{T}(\infty) - T_0 = -\frac{2}{3}\frac{\eta \bar{u}_{\mathrm{inc}}^2}{\lambda}(2T_0\alpha - 1) \tag{69}$$

or, in terms of the Eucken factor $\mathrm{Eu} = \lambda/\eta\hat{C}_V$, by

$$\bar{T}(\infty) - T_0 = -\frac{2}{3}\frac{2T_0\alpha - 1}{\mathrm{Eu}\,\hat{C}_V}\bar{u}_{\mathrm{inc}}^2 \tag{70}$$

where α is the thermal expansion coefficient of the fluid, Eq. (11), and $\bar{u}_{\mathrm{inc}}$ the mean flow velocity for an incompressible fluid in the same external circumstances, Eq. (23b). From these formulas one can calculate that the net thermal effect in a capillary flow is, in general, very small, i.e., of the order of a few millikelvins. This justifies the current assumption that the flow is isothermal. For liquids, where the compressibility parameter $C \ll 1$ so that only viscous heating occurs, the effect even turns out to be positive. However, for a capillary flow of a fluid near the gas–liquid critical point, the premise of an isothermal flow is *no* longer maintainable. This is the main conclusion of this paper. To support this statement, we have calculated the thermal effect and the corresponding entry length according to Eqs. (66) and (69) for a flow of *ethylene* at a series of densities along two supercritical isotherms, *viz.*, at 298.15 and 283.65 K. The critical parameters of ethylene are as follows: temperature $T_c = 282.35$ K, pressure $p_c = 5.040$ MPa, and density $\rho_c = 7.634\ \mathrm{kmol \cdot m^{-3}}$. A constant value of 0.1 MPa is taken for the pressure difference Δp over the capillary.

The values of the transport coefficients η and λ are derived from formulas given by Holland et al. [15] for pressures to 50 MPa, where the contribution to the thermal conductivity owing to the critical enhancement has been included. For the calculation of the quantity α, the compression factor F_c from Eq. (21) and the specific heats $\hat{C}_V$ and $\hat{C}_p$, the two IUPAC equations of state developed by Jacobsen et al. [16] have been used in and

outside the critical region, respectively. Since these two equations of state do not adjoin completely, we have corrected the calculated values slightly by applying a blending function. The mean velocity $\bar{u}_{inc}$ has been found from Eq. (23b), where use is made of the practical dimensions of a capillary as given by van den Berg et al. [6] in a description of a capillary viscometer: $R/L = 5 \times 10^{-5}$, $R = 0.04$ mm. Since the viscosity increases with the density along the isotherms, the mean velocity $\bar{u}_{inc}$ for the present capillary decreases from about 2.6 $m \cdot s^{-1}$ at low densities to 0.37 $m \cdot s^{-1}$ at $\rho = 16$ kmol $\cdot m^{-3}$. The Reynolds number varies between about 125 and 1050, and the Péclet number between about 175 and 23000, where the latter value is reached at the critical density on the nearly critical isotherm at 283.65 K, i.e., 1.3 K above T_c. The calculations demonstrate that, approaching the critical point, the parameter C and the specific heat $\hat{C}_p$ diverge more strongly than λ/η (or $Eu \cdot \hat{C}_V$), implying a substantial cooling of the flowing fluid which evolves over a drastically increased entry length ΔL_T. These effects are illustrated in Fig. 6, where the net thermal effect and the relative entry length are shown as a function of the density for the two isotherms. At 298.15 K (dashed curves) the largest thermal effect is 11 mK with an entry length of nearly 9% of the total length of the capillary. At 283.65 K (solid curves) these figures increase to 105 mK and 72%. It should be pointed out here that, due to the dependence of the thermal effect $\bar{T}(\infty) - T_0$ on the square mean velocity as given by Eq. (69), this effect is proportional to $(\Delta p)^2$ at a given temperature and density.

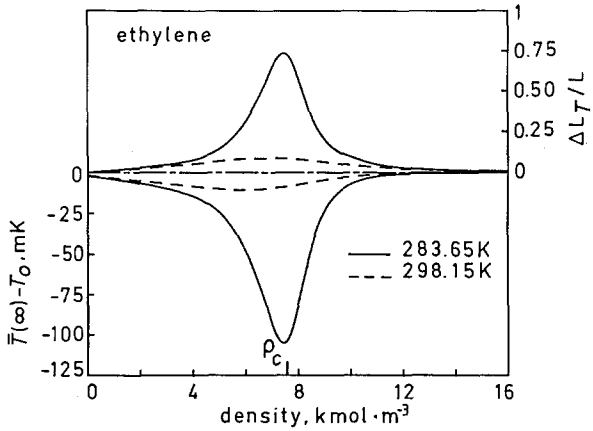

Fig. 6. The thermal effect $\bar{T}(\infty) - T_0$ and the relative entry length $\Delta L_T/L$ versus the density for a compressible capillary flow of ethylene at two supercritical temperatures. The pressure difference over the capillary is 0.1 MPa and the dimensions are $R/L = 5 \times 10^{-5}$ and $R = 4 \times 10^{-5}$ m.

With the above-mentioned capillary viscometer [6], we have performed measurements on ethylene. The corresponding experimental results will be given in a forthcoming paper, where it also will be shown that the maximum correction on the calculated viscosity due to the thermal effects amounts to about 2%. This refers to a net thermal effect of -16 mK in a flow at a temperature 1.3 K above T_c, with a mean density ρ_c, under a mean pressure difference over the capillary of about 0.04 MPa, which leads to a density range around ρ_c of nearly 30%.

5. CONCLUSIONS

In the final conclusions about the thermal effects appearing in a capillary flow, as derived in this paper, a speculation on the impact of the assumptions made in Section 2 may not be missed, in particular, of those that claim that the pressure in the capillary is a function only of the axial coordinate z and that the radial velocity u_r is zero. Concerning the validity of these assumptions, it should be pointed out here that in Ref. 1 it is shown that, in the isothermal case, the assumption $\partial p/\partial r = 0$ actually was tacitly dropped by the introduction in Eq. (14a) of the constant C_3, which is of the second order in the ratio R/L. It was also found that the ratio of pressure gradients $[\partial p/\partial(r/R)]/[\partial p/\partial(z/L)]$ is of second order and, apparently contradictory, that the ratio of the radial and axial velocity components u_r/u_z is of third order and hence negligible if only second-order terms are taken into account. Thus even if there may exist a small radial pressure gradient, the radial velocity component may be safely ignored. Therefore, in the present paper the *assumption* is made, though its validity cannot be ascertained yet, that also in the *non*isothermal case the radial velocity u_r is negligible and hence as well radial heat transport by convection.

Furthermore, it is obvious that for nearly critical circumstances, the assumption of an isothermal fluid flow, as made in Ref. 1, must be abandoned. For these circumstances, accounting for the thermal effect may, presumably, result in a significant increase in the compression factor and, consequently, in an additional nonnegligible term in the working equation for a capillary viscometer. That implies that for those circumstances and under the assumptions of a parabolic velocity profile and a constant axial pressure gradient, the results outlined here are only an estimate for the magnitude of the thermal effects. However, this estimate is most likely very reasonable in view of the fact that the velocity profile does not deviate too much from the parabolic profile for an appreciably compressible flow, as shown in Ref. 1. If the exact results are required, then the equations of motion, Eq. (8), and energy, Eq. (10), must be solved simultaneously, of course, without the two additional assumptions.

APPENDIX: BESSEL FUNCTIONS

The zero- and first-order Bessel functions $J_0(x)$ and $J_1(x)$ satisfy the relations

$$J_0(x) = \frac{1}{x} J_1(x) + J_1'(x) \tag{A1}$$

$$J_1(x) = -J_0'(x) \tag{A2}$$

Applying these relations on $I_n(\alpha)$ defined by

$$I_n(\alpha) = \int_0^1 x^n J_0(\alpha x)\, dx \qquad \text{for} \quad n = 1, 2, \ldots, \tag{A3}$$

where α is a zero of $J_0(x)$, the following recursion formulas can be derived:

$$\begin{aligned} I_1 &= \frac{1}{\alpha} J_1(\alpha) \\ I_{2n-1} &= \frac{1}{\alpha} J_1(\alpha) - \frac{4(n-1)^2}{\alpha^2} I_{2n-3} \qquad \text{for} \quad n = 2, 3, \ldots \end{aligned} \tag{A4}$$

The modulus of $J_0(\alpha x)$ is given by

$$\int_0^1 x J_0^2(\alpha x)\, dx = \tfrac{1}{2} J_1^2(\alpha) \tag{A5}$$

ACKNOWLEDGMENTS

This work, carried out at the University of Amsterdam, is supported by the "Stichting voor Fundamenteel Onderzoek der Materie (FOM)." The investigation was carried out under the auspices of the IUPAC Subcommittee on Transport Properties of Fluids. The authors wish to express their deep appreciation to Professor Kestin, the chairman of this subcommittee, for the animated and constructive discussions, which provided a valuable contribution to the development of a reliable working equation for the capillary-flow viscometer. This publication is the 411th publication of the Van der Waals Laboratory.

REFERENCES

1. H. R. van den Berg, C. A. ten Seldam, and P. S. van der Gulik, *J. Fluid Mech.* **246**:1 (1993).
2. R. K. Prud'homme, T. W. Chapman, and J. R. Bowen, *Appl. Sci. Res.* **43**:67 (1986).
3. H. C. Brinkman, *Appl. Sci. Res. A* **2**:120 (1951).

4. R. Siegel, E. M. Sparrow, and T. M. Hallman, *Appl. Sci. Res. A* 7:386 (1958).
5. H. R. van den Berg, Thesis (University of Amsterdam, Amsterdam, 1977).
6. H. R. van den Berg, C. A. ten Seldam, and P. S. van der Gulik, *Physica* **167A**:157 (1990).
7. J. Kestin and K. Pilarczyk, *Trans. Am. Soc. Mech. Eng.* **76**:987 (1954).
8. J. Kestin and H. E. Wang, *Trans. Am. Soc. Mech. Eng.* **79**:197 (1957).
9. J. Kestin and W. Leidenfrost, *Physica* **25**:1033 (1959).
10. G. Guiochon and C. L. Guillemin, *Quantitative Gas Chromatography, Journal of Chromatography Library, Vol. 42* (Elsevier Science, Amsterdam, 1988).
11. W. M. Madigosky, *J. Chem. Phys.* **46**:4441 (1967).
12. S. M. Karim and L. Rosenhead, *Rev. Mod. Phys.* **24**:108 (1952).
13. H. L. Langhaar, *J. Appl. Mech. 9 Trans. Am. Soc. Mech. Eng.* **64**:A-55 (1942).
14. R. W. Hornbeck, *Appl. Sci. Res. A* **13**:224 (1964).
15. P. M. Holland, B. E. Eaton, and H. J. M. Hanley, *J. Phys. Chem. Ref. Data* **12**:917 (1983).
16. R. T. Jacobsen, M. Jahangiri, R. B. Stewart, R. D. McCarty, J. M. H. Levelt Sengers, H. J. White, J. V. Sengers, and G. A. Olchowy, *Ethylene (Ethene), International Thermodynamic Tables of the Fluid State, Vol. 10* (Blackwell Scientific, Oxford, 1988).